Isoreticular Chiral Metal−Organic Frameworks for Asymmetric Alkene Epoxidation: Tuning Catalytic Activity by Controlling Framework Catenation and Varying Open Channel Sizes

Feijie Song, Cheng Wang, Joseph M. Falkowski, Liqing Ma, and Wenbin Lin*

Department of Chemistry, CB#3290, University of North Carolina, Chapel Hill, North Carolina 27599, United States

Received August 4, 2010; E-mail: wlin@unc.edu

Abstract: A family of isoreticular chiral metal−organic frameworks (CMOFs) of the primitive cubic network topology was constructed from $[Zn_4(\mu_4\text{-}O)(O_2CR)_6]$ secondary building units and systematically elongated dicarboxylate struts that are derived from chiral Mn-Salen catalytic subunits. CMOFs **1**−**5** were synthesized by directly incorporating three different chiral Mn-Salen struts into the frameworks under solvothermal conditions, and they were characterized by a variety of methods, including single-crystal X-ray diffraction, PXRD, TGA, and ^{1}H NMR. Although the CMOFs **1** vs **2** and CMOFs **3** vs **4** pairs were constructed from the same building blocks, they exhibit two-fold interpenetrated or non-interpenetrated structures, respectively, depending on the steric sizes of the solvents that were used to grow the MOF crystals. For CMOF-**5**, only a three-fold interpenetrated structure was obtained due to the extreme length of the Mn-Salen-derived dicarboxylate strut. The open channel and pore sizes of the CMOF series vary systematically, owing to the tunable dicarboxylate struts and controllable interpenetration patterns. CMOFs **1**−**5** were shown to be highly effective catalysts for asymmetric epoxidation of a variety of unfunctionalized olefins with up to 92% ee. The rates of epoxidation reactions strongly depend on the CMOF open channel sizes, and the catalytic activities of CMOFs **2** and **4** approach that of a homogeneous control catalyst. These results suggest that, although the diffusion of bulky alkene and oxidant reagents can be a rate-limiting factor in MOF-catalyzed asymmetric reactions, the catalytic activity of the CMOFs with large open channels (such as CMOFs **2** and **4** in the present study) is limited by the intrinsic reactivity of the catalytic molecular building blocks. The CMOF catalysts are recyclable and reusable and retain their framework structures after epoxidation reactions. This work highlights the potential of generating highly effective heterogeneous asymmetric catalysts via direct incorporation of well-defined homogeneous catalysts into framework structures of MOFs.

Introduction

Metal−organic frameworks (MOFs) have attracted a great deal of recent interest owing to the ability to fine-tune their properties at the molecular level.[1−5] Unlike traditional inorganic materials, MOFs are typically synthesized under mild conditions, allowing for the incorporation of constituent building blocks with desired functionalities, leading to numerous functional MOFs that have shown promise for a number of applications, such as gas storage,[6−9] chemical sensing,[10−14] catalysis,[15−18] biomedical imaging,[19,20] and drug delivery.[21,22] MOFs also tend to adopt ordered, crystalline structures that can be readily characterized by X-ray crystallography, which facilitates detailed elucidation of their structure−property relationships and fine-tuning of their functions. Such an ability to combine organic synthetic methodologies and crystal engineering in MOF

(1) Bradshaw, D.; Warren, J. E.; Rosseinsky, M. J. *Science* **2007**, *315*, 977.
(2) Evans, O. R.; Lin, W. *Acc. Chem. Res.* **2002**, *35*, 511.
(3) Ferey, G.; Mellot-Draznieks, C.; Serre, C.; Millange, F. *Acc. Chem. Res.* **2005**, *38*, 217.
(4) Kitagawa, S.; Kitaura, R.; Noro, S. *Angew. Chem., Int. Ed.* **2004**, *43*, 2334.
(5) Ockwig, N. W.; Delgado-Friedrichs, O.; O'Keeffe, M.; Yaghi, O. M. *Acc. Chem. Res.* **2005**, *38*, 176.
(6) Rowsell, J. L.; Yaghi, O. M. *Angew. Chem., Int. Ed.* **2005**, *44*, 4670.
(7) Kesanli, B.; Cui, Y.; Smith, M. R.; Bittner, E. W.; Bockrath, B. C.; Lin, W. B. *Angew. Chem., Int. Ed.* **2005**, *44*, 72.
(8) Dinca, M.; Long, J. R. *Angew. Chem., Int. Ed.* **2008**, *47*, 6766.
(9) Zhao, D.; Yuan, D. Q.; Zhou, H. C. *Energy Environ. Sci.* **2008**, *1*, 222.
(10) Allendorf, M. D.; Houk, R. J.; Andruszkiewicz, L.; Talin, A. A.; Pikarsky, J.; Choudhury, A.; Gall, K. A.; Hesketh, P. J. *J. Am. Chem. Soc.* **2008**, *130*, 14404.
(11) Chen, B.; Wang, L.; Xiao, Y.; Fronczek, F. R.; Xue, M.; Cui, Y.; Qian, G. *Angew. Chem., Int. Ed.* **2009**, *48*, 500.
(12) Lan, A.; Li, K.; Wu, H.; Olson, D. H.; Emge, T. J.; Ki, W.; Hong, M.; Li, J. *Angew. Chem., Int. Ed.* **2009**, *48*, 2334.
(13) Xie, Z.; Ma, L.; deKrafft, K. E.; Jin, A.; Lin, W. *J. Am. Chem. Soc.* **2010**, *132*, 922.
(14) White, K. A.; Chengelis, D. A.; Gogick, K. A.; Stehman, J.; Rosi, N. L.; Petoud, S. *J. Am. Chem. Soc.* **2009**, *131*, 18069.
(15) Kesanli, B.; Lin, W. B. *Coord. Chem. Rev.* **2003**, *246*, 305.
(16) Ingleson, M. J.; Barrio, J. P.; Bacsa, J.; Dickinson, C.; Park, H.; Rosseinsky, M. J. *Chem. Commun.* **2008**, 1287.
(17) Lee, J.; Farha, O. K.; Roberts, J.; Scheidt, K. A.; Nguyen, S. T.; Hupp, J. T. *Chem. Soc. Rev.* **2009**, *38*, 1450.
(18) Ma, L.; Abney, C.; Lin, W. *Chem. Soc. Rev.* **2009**, *38*, 1248.
(19) deKrafft, K. E.; Xie, Z.; Cao, G.; Tran, S.; Ma, L.; Zhou, O. Z.; Lin, W. *Angew. Chem., Int. Ed.* **2009**, *48*, 9901.
(20) Lin, W.; Rieter, W. J.; Taylor, K. M. *Angew. Chem., Int. Ed.* **2009**, *48*, 650.
(21) Rieter, W. J.; Pott, K. M.; Taylor, K. M.; Lin, W. *J. Am. Chem. Soc.* **2008**, *130*, 11584.
(22) Horcajada, P.; et al. *Nat. Mater.* **2010**, *9*, 172.

10.1021/ja1069773 © 2010 American Chemical Society

synthesis provides a unique opportunity for rational design and development of versatile MOFs as a new class of functional materials.

Because of their mild synthetic conditions, MOFs are particularly suited for immobilizing well-defined molecular catalysts, leading to a new generation of solid catalysts with uniform catalytic sites and open channel structures for shape-, size-, chemo-, and enantioselective reactions. The ability to easily recover and reuse such MOF-based heterogeneous catalysts is also highly desirable for reducing processing and waste disposal costs in large-scale reactions. Compared to other immobilized catalytic systems, MOFs can have well-defined, single-crystalline solid structures, unprecedentedly high catalyst loadings, more uniform and accessible catalytic centers, and enhanced catalytic activity by eliminating multimolecular catalyst deactivation pathways.[15,17,18]

Although a large number of MOFs have been examined as heterogeneous catalysts, most of these studies rely on the intrinsic catalytic activity (e.g., weak Lewis acidity) of the metal-connecting points.[15,17,23−25] A more rational strategy than such an "opportunistic" approach is to introduce well-defined molecular catalysts into the MOF structures,[15,18,23,25] which can lead to a new generation of heterogeneous catalysts that are capable of catalyzing more advanced and value-added reactions, such as enantioselective reactions. Post-synthesis modification (PSM) has recently been successfully used to generate highly active and selective MOF catalysts,[26−28] but this method tends to reduce the open channel sizes during the PSM process and hence negatively impacts the performance of MOF catalysts by slowing down substrate and product diffusion through the channels. Direct incorporation of a well-defined homogeneous catalyst (or precatalyst) into the framework of a MOF represents an attractive alternative that has so far been under-explored.[29−31] We report here the rational design of a family of isoreticular chiral MOFs based on Mn-Salen-derived bridging ligands and the applications of these solid catalysts in highly enantioselective alkene epoxidation reactions.
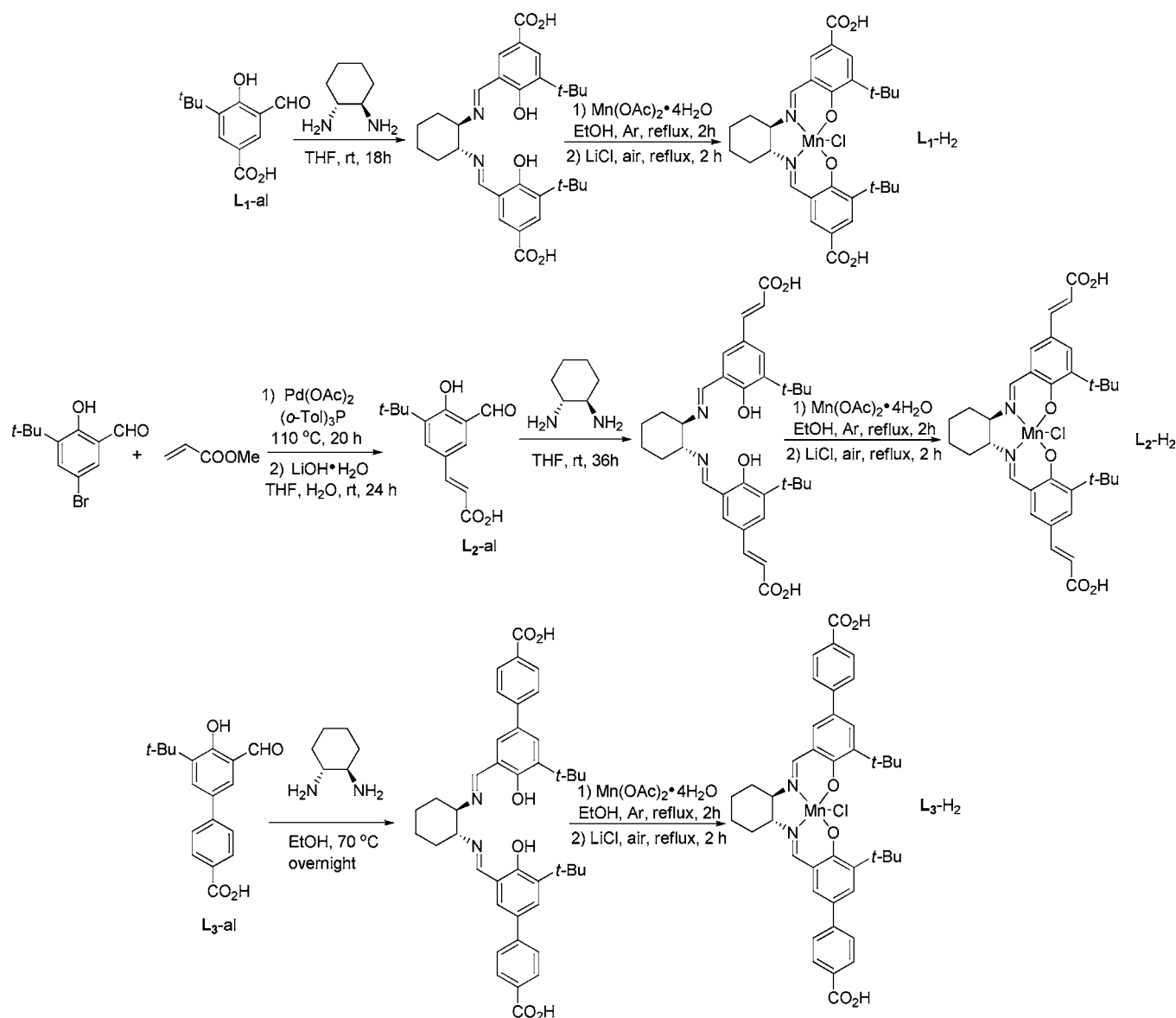
Isoreticular MOFs with the same framework topology but tunable pore and channel sizes have been constructed by linking metal-coordinated secondary building units (SBUs) with bridging ligands of varied length.[32−43] Among the many metal-coordinated SBUs, $[Zn_4(\mu_4\text{-O})(O_2CR)_6]$,[36,37] $[Cu_2(sol)_2(O_2CR)_4]$,[38−41] and $[Zr_6(O)_4(OH)_4(O_2CR)_{12}]$[42,43] are most commonly used for con-

structing isoreticular MOFs. These sterically demanding SBUs have been shown to sustain non-interpenetrated MOF structures, but the tendency to form interpenetrated networks increases as the bridging ligands become longer. Such interpenetrations can severely reduce or even eliminate the interior void space of the MOFs. A few reports have recently appeared on controlling framework catenation by varying reaction temperature or reagent concentration,[36,44] templating with oxalic acid,[45] introducing space-filling groups on the ligands,[46] and employing solvent molecules of different sizes as templates.[39]

In this work, we hypothesize that isoreticular chiral MOFs (CMOFs) of tunable open channel sizes can be constructed from $[Zn_4(\mu_4\text{-O})(O_2CR)_6]$ SBUs and tunable Mn-Salen-derived dicarboxylic acids. Chiral Salen ligands, such as (R,R)-1,2-cyclohexanediamino-N,N′-bis(3-*tert*-butyl-salicylidene), have been established as one of the few privileged ligand systems for asymmetric catalysis.[47] Mn-Salen complexes have, for example, been shown to be highly effective in catalyzing asymmetric epoxidation reactions of unfunctionalized olefins.[48−54] Several reports have used Salen-type ligands to construct MOFs.[55−57] For example, Kitagawa et al. synthesized an achiral Zn-MOF using M-salphdc (M = Cu(II), Co(II), and Ni(II); salphdc = N,N′-phenylenebis(salicylideneimine)dicarboxylic acid) building blocks,[58] whereas Chen et al. studied hydrogen uptake with mixed metal MOFs constructed from the achiral Cu(Pyen) structure (Pyen-H_2 = 5-methyl-4-oxo-1,4-dihydro-pyridine-3-carbaldehyde).[59] Mirkin et al. studied the interconversion between amorphous and crystalline microparticles that are built from Ni-salen-dicarboxylic acid and an excess amount of Ni(OAc)$_2$·4H$_2$O.[56] Cui et al. carried out chiral recognition and separation using a 2-D coordination polymer built from unsymmetrical chiral Schiff base metal complexes.[60] Hupp et al. constructed a chiral MOF based on the Mn-Salen-derived

(23) Lin, W. B. *J. Solid State Chem.* **2005**, *178*, 2486.
(24) Wang, Z.; Chen, G.; Ding, K. L. *Chem. Rev.* **2009**, *109*, 322.
(25) Lin, W. B. *MRS Bull.* **2007**, *32*, 544.
(26) Wu, C. D.; Hu, A.; Zhang, L.; Lin, W. *J. Am. Chem. Soc.* **2005**, *127*, 8940.
(27) Banerjee, M.; Das, S.; Yoon, M.; Choi, H. J.; Hyun, M. H.; Park, S. M.; Seo, G.; Kim, K. *J. Am. Chem. Soc.* **2009**, *131*, 7524.
(28) Tanabe, K. K.; Cohen, S. M. *Angew. Chem., Int. Ed.* **2009**, *48*, 7424.
(29) Hu, A.; Ngo, H. L.; Lin, W. *J. Am. Chem. Soc.* **2003**, *125*, 11490.
(30) Hu, A.; Ngo, H. L.; Lin, W. *Angew. Chem., Int. Ed.* **2003**, *42*, 6000.
(31) Cho, S. H.; Ma, B.; Nguyen, S. T.; Hupp, J. T.; Albrecht-Schmitt, T. E. *Chem. Commun.* **2006**, 2563.
(32) Lin, W. B.; Evans, O. R.; Xiong, R. G.; Wang, Z. Y. *J. Am. Chem. Soc.* **1998**, *120*, 13272.
(33) Evans, O. R.; Xiong, R. G.; Wang, Z. Y.; Wong, G. K.; Lin, W. B. *Angew. Chem., Int. Ed.* **1999**, *38*, 536.
(34) Evans, O. R.; Lin, W. B. *Chem. Mater.* **2001**, *13*, 3009.
(35) Evans, O. R.; Lin, W. B. *Chem. Mater.* **2001**, *13*, 2705.
(36) Eddaoudi, M.; Kim, J.; Rosi, N.; Vodak, D.; Wachter, J.; O'Keeffe, M.; Yaghi, O. M. *Science* **2002**, *295*, 469.
(37) Li, Q.; Zhang, W.; Miljanic, O. S.; Sue, C. H.; Zhao, Y. L.; Liu, L.; Knobler, C. B.; Stoddart, J. F.; Yaghi, O. M. *Science* **2009**, *325*, 855.
(38) Ma, L.; Lee, J. Y.; Li, J.; Lin, W. *Inorg. Chem.* **2008**, *47*, 3955.
(39) Ma, L.; Lin, W. *J. Am. Chem. Soc.* **2008**, *130*, 13834.

(40) Lin, X.; Telepeni, I.; Blake, A. J.; Dailly, A.; Brown, C. M.; Simmons, J. M.; Zoppi, M.; Walker, G. S.; Thomas, K. M.; Mays, T. J.; Hubberstey, P.; Champness, N. R.; Schroder, M. *J. Am. Chem. Soc.* **2009**, *131*, 2159.
(41) Wu, S.; Ma, L.; Long, L. S.; Zheng, L. S.; Lin, W. *Inorg. Chem.* **2009**, *48*, 2436.
(42) Cavka, J. H.; Jakobsen, S.; Olsbye, U.; Guillou, N.; Lamberti, C.; Bordiga, S.; Lillerud, K. P. *J. Am. Chem. Soc.* **2008**, *130*, 13850.
(43) Guillerm, V.; Gross, S.; Serre, C.; Devic, T.; Bauer, M.; Ferey, G. *Chem. Commun.* **2010**, *46*, 767.
(44) Zhang, J.; Wojtas, L.; Larsen, R. W.; Eddaoudi, M.; Zaworotko, M. J. *J. Am. Chem. Soc.* **2009**, *131*, 17040.
(45) Ma, S.; Sun, D.; Ambrogio, M.; Fillinger, J. A.; Parkin, S.; Zhou, H. C. *J. Am. Chem. Soc.* **2007**, *129*, 1858.
(46) Farha, O. K.; Malliakas, C. D.; Kanatzidis, M. G.; Hupp, J. T. *J. Am. Chem. Soc.* **2010**, *132*, 950.
(47) Yoon, T. P.; Jacobsen, E. N. *Science* **2003**, *299*, 1691.
(48) Palucki, M.; Finney, N. S.; Pospisil, P. J.; Guler, M. L.; Ishida, T.; Jacobsen, E. N. *J. Am. Chem. Soc.* **1998**, *120*, 948.
(49) Zhang, W.; Loebach, J. L.; Wilson, S. R.; Jacobsen, E. N. *J. Am. Chem. Soc.* **1990**, *112*, 2801.
(50) Katsuki, T. *Synlett* **2003**, 281–297.
(51) Venkataramanan, N. S.; Kuppuraj, G.; Rajagopal, S. *Coord. Chem. Rev.* **2005**, *249*, 1249.
(52) Baleizao, C.; Garcia, H. *Chem. Rev.* **2006**, *106*, 3987–4043.
(53) Canali, L.; Sherrington, D. C. *Chem. Soc. Rev.* **1999**, *28*, 85.
(54) Gupta, K. C.; Sutar, A. K.; Lin, C. C. *Coord. Chem. Rev.* **2009**, *253*, 1926.
(55) Oh, M.; Mirkin, C. A. *Angew. Chem., Int. Ed.* **2006**, *45*, 5492.
(56) Jeon, Y. M.; Heo, J.; Mirkin, C. A. *J. Am. Chem. Soc.* **2007**, *129*, 7480.
(57) Jung, S.; Oh, M. *Angew. Chem., Int. Ed.* **2008**, *47*, 2049.
(58) Kitaura, R.; Onoyama, G.; Sakamoto, H.; Matsuda, R.; Noro, S.; Kitagawa, S. *Angew. Chem., Int. Ed.* **2004**, *43*, 2684.
(59) Chen, B.; Zhao, X.; Putkham, A.; Hong, K.; Lobkovsky, E. B.; Hurtado, E. J.; Fletcher, A. J.; Thomas, K. M. *J. Am. Chem. Soc.* **2008**, *130*, 6411.
(60) Yuan, G.; Zhu, C.; Xuan, W.; Cui, Y. *Chemistry* **2009**, *15*, 6428.

Scheme 1. Synthesis of Ligands L_1-H_2−L_3-H_2

bipyridine bridging ligand and demonstrated its asymmetric catalytic activity in alkene epoxidation reactions, albeit at lower enantioselectivity than the homogeneous counterpart.[31] However, no systematic study on constructing isoreticular Mn-Salen-based MOFs with tunable open channels has appeared in the literature to date.

Systematic tuning of highly porous MOFs for gas storage applications elucidated the relationships between channel opening sizes/framework interpenetrations and gas-uptake capacities of MOFs.[7,45,59,61,62] On the other hand, there is only one study on the dependence of MOF catalytic properties on the open channel sizes.[63] In this paper, we not only develop a family of isoreticular CMOFs based on $[Zn_4(\mu_4\text{-}O)(O_2CR)_6]$ SBUs and tunable Mn-Salen-derived dicarboxylic acids but also demonstrate the control over framework catenation using solvents of different steric bulk and the dependence of MOF enantioselec-

tive alkene epoxidation catalytic activity on framework catenation and open channel sizes. Our work provides solid evidence that the catalytic activity of the CMOFs with large open channels can rival that of an analogous homogeneous catalyst and is limited by the intrinsic reactivity of the catalytic molecular building blocks.
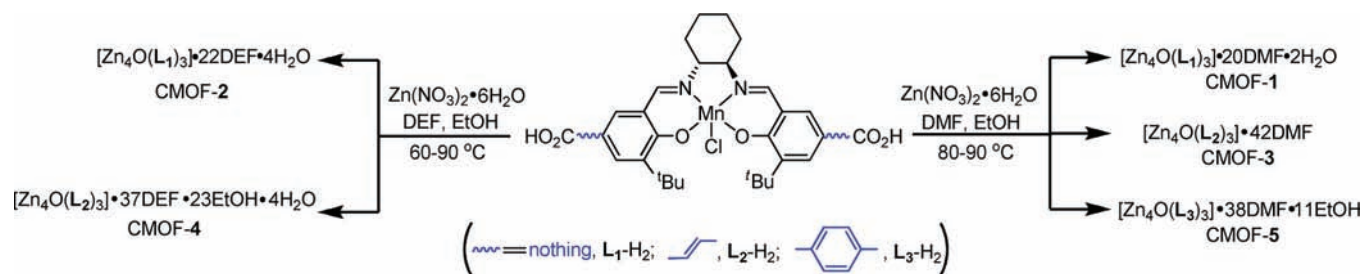
Results and Discussion

Synthesis and Characterization. Enantiopure Mn-Salen dicarboxylic acid ligands, L_1-H_2 to L_3-H_2, were synthesized by Schiff base condensation reactions between (R,R)-cyclohexanediamine and corresponding 2-hydroxybenzaldehyde derivatives with pendant carboxylic acid groups (L_1-al to L_3-al), followed by metalation with $Mn(OAc)_2\cdot4H_2O$ and in situ oxidation in air to afford Mn(III) complexes (Scheme 1). The 2-hydroxybenzaldehyde derivatives L_1-al and L_3-al are known compounds, whereas L_2-al was synthesized by a Pd-catalyzed carbon−carbon coupling reaction between the bromo compound and methyl acrylate followed by base-promoted hydrolysis. More detailed synthetic schemes and procedures are shown in

(61) Ryan, P.; Broadbelt, L. J.; Snurr, R. Q. *Chem. Commun.* **2008**, 4132.
(62) Wang, Z.; Tanabe, K. K.; Cohen, S. M. *Chemistry* **2010**, *16*, 212.
(63) Ma, L.; Falkowski, J. M.; Abney, C.; Lin, W. *Nat. Chem.* **2010**, *2*, 838–846.

Scheme 2. Synthesis of CMOFs **1**−**5**

the Supporting Information. All of the new compounds were characterized by NMR spectroscopy and mass spectrometry.

We hypothesized that Mn-Salen-derived dicarboxylate ligands L_1−L_3 can link octahedral $[Zn_4(\mu_4\text{-}O)(O_2CR)_6]$ SBUs to form isoreticular CMOFs of the primitive cubic network (pcu) topology with tunable pore/channel sizes and shapes. As shown in Scheme 2, reactions of $Zn(NO_3)_2 \cdot 6H_2O$ with the Mn-Salen complex L_1-H_2 in dimethylformamide (DMF)/EtOH at 80−90 °C for 96 h afforded dark brown single crystals of $[Zn_4(\mu_4\text{-}O)(L_1)_3] \cdot 20DMF \cdot 2H_2O$ (CMOF-**1**). CMOF-**1** crystallizes in the trigonal $R32$ space group, as revealed by single-crystal X-ray crystallography (Figures 1 and 2). The asymmetric unit of the CMOF-**1** framework contains two L_1 ligands, two-thirds of $Zn_4(\mu_4\text{-}O)$ clusters which are composed of two Zn atoms of full occupancy and two Zn atoms of one-third occupancy, and two O atoms of one-third occupancy. As expected, the carboxylate groups from six adjacent L_1 ligands coordinate to the four Zn centers to form $[Zn_4(\mu_4\text{-}O)(carboxylate)_6]$ SBUs, which link L_1 ligands to form a 3D network of the pcu topology. Because of the elongated L_1 ligands, CMOF-**1** adopts a two-fold interpenetrated structure with 61.1% of void space as calculated by PLATON that is filled by the DMF and water molecules.[64] The precise solvent content cannot be determined by X-ray crystallography owing to their disordered nature. The solvent contents were instead established by a combination of ^1H NMR studies and thermogravimetric analysis (Supporting Information). The largest dimensions of open channels measure 0.8×0.6 nm^2, and the largest cavities inside the interpenetrated networks measure 1.4 nm in diameter in CMOF-**1** (Figure 3).

As we have shown previously,[39] catenation isomerism can be controlled by introducing solvent molecules of different sizes
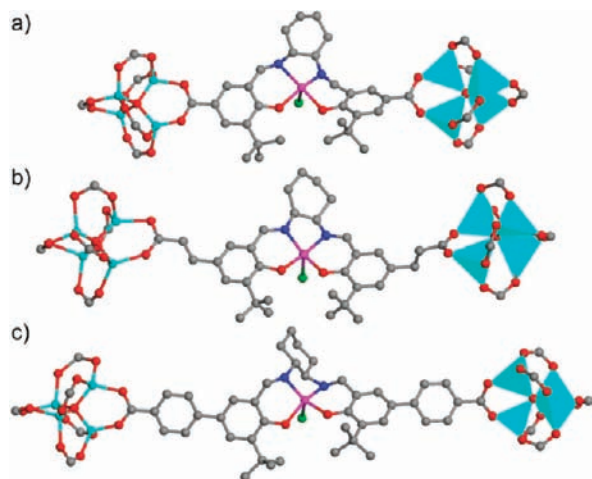

Figure 1. Ball-and-stick and polyhedra presentations of Mn-Salen-derived dicarboxylate bridging ligands L_1 (a), L_2 (b), and L_3 (c) and the $[Zn_4O(carboxylate)_6]$ SBUs in CMOFs **1**−**5**.

which act as space-filling templates. Diethylformamide (DEF) is a larger molecule than DMF and thus can favor the formation of non-interpenetrated structure as a result of the solvent templating effects. When the reaction between $Zn(NO_3)_2 \cdot 6H_2O$ and L_1-H_2 was carried out in DEF/EtOH at 60−90 °C, the non-interpenetrated 3D CMOF-**2** was obtained, with the formula determined to be $[Zn_4(\mu_4\text{-}O)(L_1)_3] \cdot 22DEF \cdot 4H_2O$ (Scheme 2). Single-crystal X-ray crystallography showed that CMOF-**2** has cell parameters very similar to those of CMOF-**1** but crystallizes in the space group $R3$. The framework of CMOF-**2** is exactly identical to one of the two interpenetrating nets in CMOF-**1**, with the same metal−ligand connectivity and network topology (Figure 2). The non-interpenetrated framework enjoys much larger open channel dimensions of 2.0×1.6 nm^2 and a cavity size of 2.6 nm (Figure 3), with 80.2% of void space as calculated by PLATON. This huge enhancement of accessible internal volume and open channel size in non-interpenetrated structures is crucial for enhanced catalytic performance by facilitating the diffusion of reactants and products (see below).

Similar reactions of $Zn(NO_3)_2 \cdot 6H_2O$ with L_2-H_2 in DMF/ EtOH and DEF/EtOH resulted in single crystals of $[Zn_4(\mu_4\text{-}O)(L_2)_3] \cdot 42DMF$ (CMOF-**3**) and $[Zn_4(\mu_4\text{-}O)(L_2)_3] \cdot 37DEF \cdot 23EtOH \cdot 4H_2O$ (CMOF-**4**), respectively (Scheme 2). Just as in the CMOF-**1**/**2** pair, CMOF-**3** and CMOF-**4** adopt two-fold interpenetrated and non-interpenetrated structure, respectively (Figure 2). The two-fold interpenetrated CMOF-**3** possesses channel sizes of 1.5×0.7 nm^2 and an open cavity of 2.0 nm in diameter, with 76.8% of void space, while the non-interpenetrated CMOF-**4** exhibits the largest channel dimensions of 2.5×2.3 nm^2 and a cavity diameter of 3.2 nm (Figure 3), reaching 88.4% of void space as calculated by PLATON. The synthesis of CMOF-**1** vs -**2** or CMOF-**3** vs -**4** is dependent on the steric bulk of the templating solvents but does not appear to be sensitive to the reaction/crystallization temperatures. For example, CMOF-**4** was obtained in pure phase in the 60−90 °C temperature range, but as expected, longer reaction time was needed for the reactions carried out at lower temperatures.

As ligand L_3 gets even longer, the reactions between L_3-H_2 and $Zn(NO_3)_2$ in both DMF/EtOH and DEF/EtOH yield the same interpenetrated framework, CMOF-**5** (Scheme 2). Similar reactions in even more sterically demanding solvents such as N,N'-dibutylformamide and N,N'-diisopropylformamide also failed to produce non-interpenetrated CMOF, implying a delicate balance between framework catenation and solvent templating effects. CMOF-**5** grown in DMF at 80 °C has the formula of $[Zn_4(\mu_4\text{-}O)(L_3)_3] \cdot 38DMF \cdot 11EtOH$. Unlike CMOF-**1** or CMOF-**3**, CMOF-**5** adopts a three-fold interpenetrated framework that crystallizes in the $R3$ space group (Figure 2). Detailed analysis of the single-crystal X-ray diffraction data revealed that two of the three interpenetrating nets are fully occupied and pack closely to each other, while the third fold randomly occupies
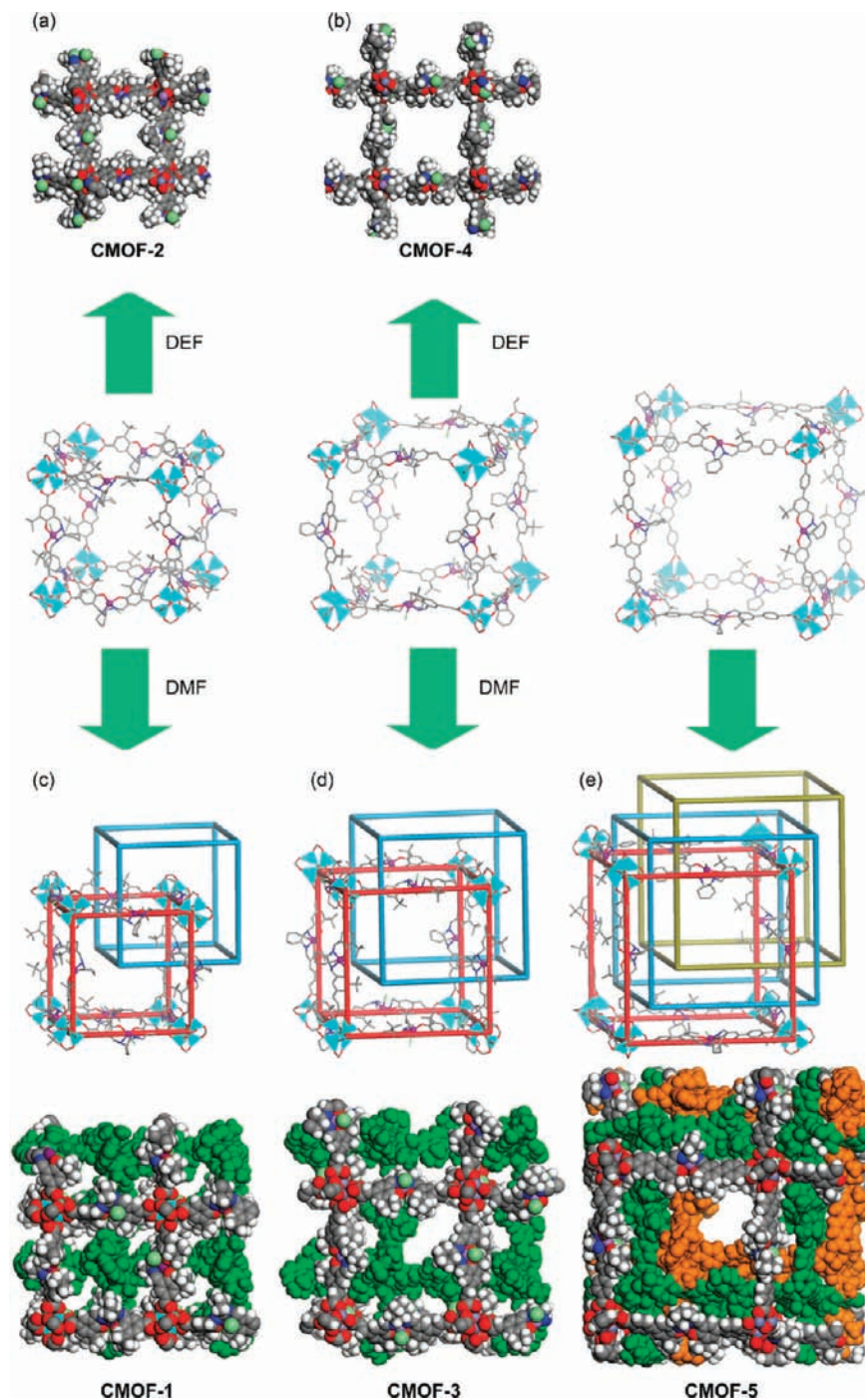
Figure 2. Stick/polyhedra models showing the connectivity of Mn-Salen-derived dicarboxylate bridging ligands (L_1–L_3) and [$Zn_4O(carboxylate)_6$] SBUs and the interpenetration of the pcu networks and space-filling models as viewed perpendicular to the (1 0 −2) plane in (a) CMOF-**2** (one-fold), (b) CMOF-**4** (one-fold), (c) CMOF-**1** (two-fold), (d) CMOF-**3** (two-fold), and (e) CMOF-**5** (three-fold).

three possible positions with a one-third occupancy (Supporting Information). The assignment of three-fold interpenetration is fully supported by the ^1H NMR and TGA solvent content measurements in combination with the void space predicted from the structural model. In a simplified model of three closely packed and fully occupied interpenetrating nets, CMOF-**5** possesses open channel (1.1×0.8 nm^2) and cavity (1.8 nm) dimensions that are intermediate between those of CMOF-**1** and CMOF-**3** (Figure 3). Phase purity of the bulky crystalline samples of all the five CMOFs was confirmed by an excellent

match between the experimental and simulated powder X-ray diffraction (PXRD) patterns.

Although interpenetration is frequently encountered in the literature, few methods other than time-consuming single-crystal X-ray crystallography can tell the difference between interpenetrated and non-interpenetrated structures. PXRD patterns of interpenetrated and non-interpenetrated structures often do not differ much, and cannot be used as a reliable indicator for framework catenation (see below). The density of MOF crystals
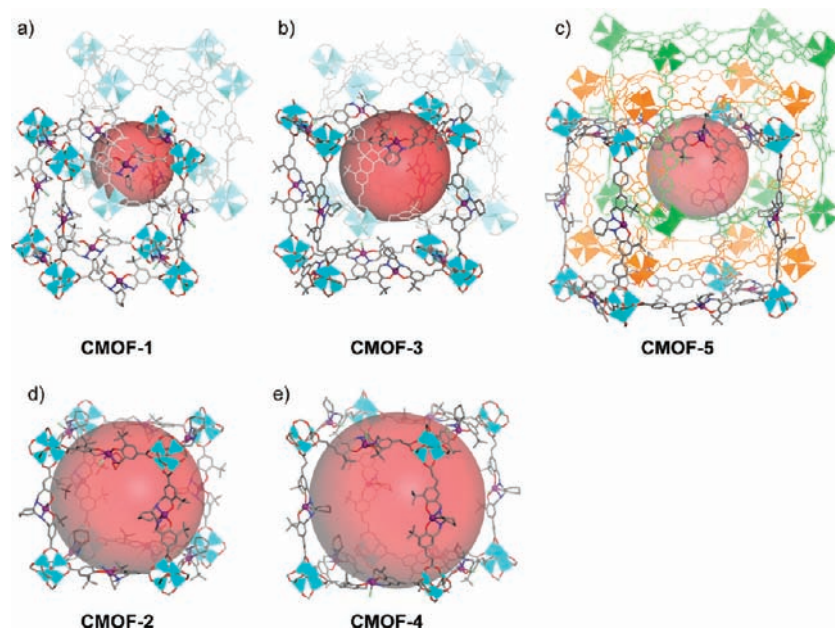
Figure 3. Different cavity sizes shown as red balls in CMOFs **1**−**5**: (a) CMOF-**1** (1.4 nm); (b) CMOF-**3** (2.0 nm); (c) CMOF-**5** (1.8 nm); (d) CMOF-**2** (2.6 nm); (e) CMOF-**4** (3.2 nm).
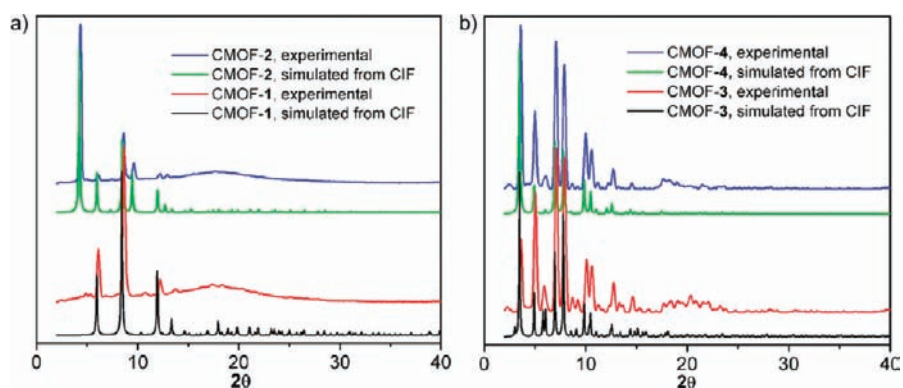

Figure 4. Powder X-ray diffraction patterns for (a) CMOF-**1** simulated from CIF file (black), CMOF-**1** as synthesized (red), CMOF-**2** simulated from CIF file (green), CMOF-**2** as synthesized (blue); (b) CMOF-**3** simulated from CIF file (black), CMOF-**3** as synthesized (red), CMOF-**4** simulated from CIF file (green), CMOF-**4** as synthesized (blue).

can be a potentially useful indicator for framework catenation,[65] but when the channel sizes of MOFs are very large, as in this CMOF series, solvent molecules used for density measurements can exchange with the native solvent molecules to alter the crystal density and to render this technique useless. The determination of included solvent molecules inside MOF channels, although not very precise, provides a simple and reliable way to identify different interpenetration patterns in the bulk samples and to provide supporting evidence to the single-crystal X-ray diffraction results.

From single-crystal structures, the relative positions of the two interpenetrating nets in CMOF-**1** and CMOF-**3** are different. In CMOF-**1**, each net sits right in the middle of the other, whereas in CMOF-**3**, the second fold of the nets resides off the center of the first one (Figure 2). The relative positions of the two nets in the interpenetrated structures of CMOF-**1** and CMOF-**3** are supported by the PXRD studies. Comparing the

(64) Spek, A. L. *J. Appl. Crystallogr.* **2003**, *36*, 7.
(65) Farha, O. K.; Mulfort, K. L.; Thorsness, A. M.; Hupp, J. T. *J. Am. Chem. Soc.* **2008**, *130*, 8598.

PXRD patterns of CMOF-**1** and CMOF-**2**, the first peak around $2\theta = 4.3°$ in the powder pattern of CMOF-**2** (corresponding to the Miller indices 1 0 −2) is absent in that of CMOF-**1** (Figure 4a). The absence of the 1 0 −2 peak can occur only when the second fold of the nets sits right in the middle of the first fold, which generates a pseudo 4_3 screw axis for the $[Zn_4(\mu_4\text{-}O)(\text{carboxylate})_6]$ SBUs and hence introduces additional systematic absence. In contrast, comparing the PXRD patterns of CMOF-**3** and CMOF-**4**, no additional absence is observed for CMOF-**3**, while peak intensities do change with respect to that of CMOF-**4** (Figure 4b). It is important to note that the relative positions of the two interpenetrating nets also significantly modify the maximum open channel sizes and accessible cavity volumes in the structures.

High porosity, which is needed to efficiently transport reagent and product molecules to facilitate asymmetric catalysis, was expected for all the CMOFs **1**−**5** on the basis of the crystal structures. However, nitrogen adsorption measurements indicated that the CMOFs exhibit negligible surface areas. The discrepancy between expected and experimental surface areas

Table 1. Key Crystallographic and Dye Uptake Data for CMOFs **1**−**5**

	CMOF-**1**	CMOF-**2**	CMOF-**3**	CMOF-**4**	CMOF-**5**
framework formula	$[Zn_4O(L_1)_3]$	$[Zn_4O(L_1)_3]$	$[Zn_4O(L_2)_3]$	$[Zn_4O(L_2)_3]$	$[Zn_4O(L_3)_3]$
space group	*R*32	*R*3	*R*32	*R*3	*R*3
cell dimensions (Å)	29.7 × 29.7 × 72.7	29.6 × 29.6 × 72.5	35.9 × 35.9 × 87.8	35.9 × 35.9 × 87.9	41.9 × 41.9 × 100.3
interpenetration	two-fold	one-fold	two-fold	one-fold	three-fold
void space % calcd by PLATON	61.1	80.2	76.8	88.4	75.9
framework density (g/cm^3)	0.758	0.382	0.462	0.230	0.502
largest channel sizes (nm)	0.8 × 0.6	2.0 × 1.6	1.5 × 0.7	2.5 × 2.3	1.1 × 0.8
largest cavity (nm)	1.4	2.6	2.0	3.2	1.8
solvent content[a]	20DMF·2H$_2$O	22DEF·4H$_2$O	42DMF	37DEF·23EtOH·4H$_2$O	38DMF·11EtOH
solvent weight loss (%)[b]	41.3	53.2	55.5	68.1	53.0
dye uptake (wt % of the framework)	2.1	15.4	6.3	37.7	16.3
effective dye concentration inside MOF channels (mM)	31.1	90.0	45.6	152.1	125.0

[a] Solvent contents were determined by a combination of ^1H NMR spectroscopy and TGA. [b] The solvent weight loss happened in the 25−250 °C temperature range.

probably results from the framework distortion upon solvent removal, a phenomenon commonly observed for MOFs with large open channels.[66−69] This was confirmed by PXRD studies of the evacuated sample of CMOF-**2**, showing the loss of ordered framework structure after removing the solvents. On the other hand, the test for the accessibility of MOF channels to solvent or other large molecules is more relevant to screening heterogeneous asymmetric catalysts, as enantioselective organic transformations are typically carried out in solution. A dye uptake assay recently developed in our laboratory[63] was thus employed to quantify the intrinsic porosity of the CMOFs as well as the capability of the channels in transporting large molecules. By soaking the CMOFs in a solution of 24.2 mM Brilliant Blue R-250 (BBR-250) dye in methanol for 16 h, significant fractions of the BBR-250 can be absorbed into the internal channels of the CMOFs. The dye solution was then decanted, and the CMOFs were washed with water several times to remove dye molecules adsorbed on the external surfaces of the crystals. The dye-loaded CMOFs were then digested with disodium ethylenediaminetetraacetate (Na$_2$EDTA), and the amounts of released BBR-250 were quantified by ultraviolet−visible spectroscopy. As shown in Table 1, the CMOF series exhibit dye uptake capacity (ranging from 2.1 to 37.7 wt % of the framework) dependent upon the open channels, corresponding to an effective dye concentration of 31.1−152.1 mM in the channels of the CMOFs, which is equivalent to 1.3−6.3 times the original dye concentration in the MeOH solution. These results unambiguously prove the accessibility of the open channels of the CMOFs to large reagents typically used for enantioselective catalysis, as the BBR-250 molecule has an estimated cross section of 1.8 × 2.2 nm^2. Moreover, the drastic difference in dye uptake capacities between interpenetrated and non-interpenetrated CMOFs (2.1 wt % for **1** vs 15.4 wt % for **2** and 6.3 wt % for **3** vs 37.7 wt % for **4**) provides another important means for identifying framework catenation.

Isoreticular MOFs based on $[Zn_4(\mu_4\text{-}O)(O_2CR)_6]$ SBUs represent the most well-established family of isoreticular porous materials. The CMOF series represents the first isoreticular MOFs that are built from direct incorporation of catalytically

competent bridging ligands.[63] With the ease of changing the length of two-connected linear dicarboxylate bridging ligands, the channel and cavity sizes of the resulting MOFs can be systematically tuned. Controlling interpenetrations with the help of templating solvents provides an additional means to alter the open channel sizes. The successful incorporation of molecular Mn-Salen catalytic building blocks into the 3D frameworks and the tunable open channel and pore sizes of this CMOF series open up a great opportunity toward delineating their structure/catalytic activity relationships in enantioselective alkene epoxidation reactions.

Enantioselective Catalysis. Catalytic activities of CMOFs **1**−**5** toward asymmetric epoxidation of unfunctionalized olefins were evaluated with 1*H*-indene (**6a**) as substrate and 2-(*tert*-butylsulfonyl)iodosylbenzene (**7**) as oxidant. As shown in Table 2 (entries 1−3), CMOFs **1**, **3**, and **5** are highly effective catalysts for asymmetric epoxidation of **6a** to generate (1*R*,2*S*)-indene oxide in 47−64% ee. In comparison, the homogeneous control, **L$_3$**-Me$_2$, gave (1*R*,2*S*)-indene oxide in 64% ee. The conversions of **6a** range from 54% to 80% for CMOFs **1**, **3**, and **5**, which compare favorably with that of the homogeneous control **L$_3$**-Me$_2$ (60%, Table 1, entry 4). CMOF-**4** and CMOF-**5** have also been shown to be highly effective in asymmetric epoxidation of a variety of unfucntionalized alkenes to afford chiral epoxides in good to excellent yields and ee's (Table 2), demonstrating generality of the asymmetric epoxidation activities of CMOF catalysts. The level of enantioselectivity observed for CMOF-catalyzed alkene epoxidation is comparable to that of the homogeneous control catalyst **L$_3$**-Me$_2$. Asymmetric epoxidation of 2,2-dimethyl-2*H*-chromene (**6b**) by CMOF-**5**, for example, gave the (*R*,*R*)-chromene oxide in 92% ee, a value that is the same as the homogeneous result for **L$_3$**-Me$_2$ and higher than the ee value (82%) reported earlier for a chiral MOF built from (*R*,*R*)-1,2-cyclohexanediamino-*N*,*N*′-bis(3-*tert*-butyl-5-(4-pyridyl)salicylidene)Mn^{III}Cl.[31]
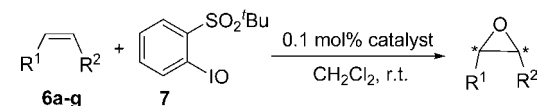
The isoreticular nature of CMOFs **1**−**5** provides an interesting platform for probing the dependence of epoxidation reaction rates on the open channel dimensions. As shown in Figure 5, the time-dependent conversion curves for the epoxidation of **6b** greatly depend on the channel sizes. The conversion rate increases in the order of CMOF-**1** < CMOF-**5** < CMOF-**3** < CMOF-**2** < CMOF-**4**, consistent with the increase of open channel sizes in this series (Table 1). This trend suggests that the diffusion of the bulky alkene and oxidant reagents and the epoxide product can be a significant factor in determining the reaction rates for CMOF-catalyzed asymmetric epoxidation
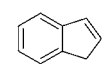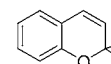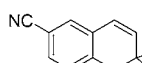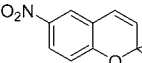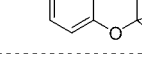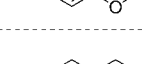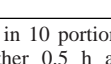
(66) Serre, C.; Millange, F.; Thouvenot, C.; Nogues, M.; Marsolier, G.; Louer, D.; Ferey, G. *J. Am. Chem. Soc.* **2002**, *124*, 13519.
(67) Ghoufi, A.; Maurin, G. *J. Phys. Chem. C* **2010**, *114*, 6496.
(68) Llewellyn, P. L.; Maurin, G.; Devic, T.; Loera-Serna, S.; Rosenbach, N.; Serre, C.; Bourrelly, S.; Horcajada, P.; Filinchuk, Y.; Ferey, G. *J. Am. Chem. Soc.* **2008**, *130*, 12808.
(69) Neimark, A. V.; Coudert, F. X.; Boutin, A.; Fuchs, A. H. *J. Phys. Chem. Lett.* **2010**, *1*, 445.

Table 2. CMOF-Catalyzed Enantioselective Epoxidation of Alkenes[a]

entry	catalyst	alkene		conv.%[b]	ee%[c]
1	CMOF-**1**			63	47
2	CMOF-**3**		**6a**	80	64
3	CMOF-**5**			54	61
4	L₃-Me₂			60	64
5	CMOF-**5**			82	92
6	CMOF-**4**		**6b**	87	85
7	L₃-Me₂			90	92
8	CMOF-**5**			60	79
9	CMOF-**4**		**6c**	79	83
10	L₃-Me₂			82	88
11	CMOF-**4**		**6d**	93	81
12	L₃-Me₂			97	88
13	CMOF-**4**		**6e**	89	77
14	L₃-Me₂			80	87
15	CMOF-**4**		**6f**	79	75
16	L₃-Me₂			81	88
17	CMOF-**5**			>99	42
18	CMOF-**4**		**6g**	>99	39
19	L₃-Me₂			>99	45

[a] 0.5 equiv of oxidants added in 10 portions at 15 min intervals, and the reaction continued for another 0.5 h after the oxidant addition. [b] Determined by GC. [c] Determined by chiral GC with a Supelco β-DEX 120 capillary column or by chiral HPLC with a Chiralcel AD column.
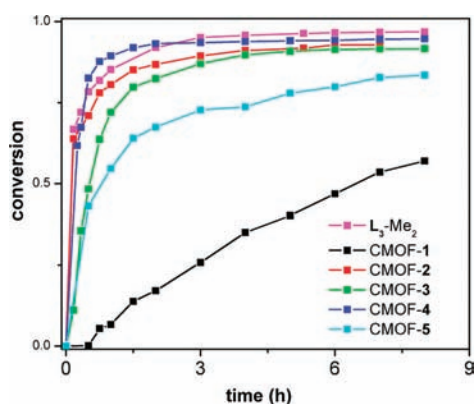

Figure 5. Plots of percent conversions versus time for epoxidation of 2,2-dimethyl-2H-chromene catalyzed by CMOF-**1** (black), CMOF-**2** (red), CMOF-**3** (green), CMOF-**4** (blue), CMOF-**5** (cyan), and **L₃-Me₂** (purple). The epoxidation reactions were carried out with 3 equiv of 2-(tert-butylsulfonyl)iodosylbenzene in the presence of 0.1 mol % catalyst.
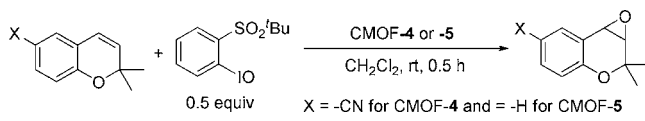
reactions when the CMOF channels are small (as in interpenetrated CMOFs **1**, **3**, and **5**). On the other hand, CMOF-**2** and CMOF-**4** gave conversion rates comparable to that of the homogeneous catalyst **L₃-Me₂**, suggesting that the substrate and

product diffusion through open channels is not the rate-limiting factor. With open channel sizes of 2.0×1.6 nm² and 2.5×2.3 nm² in CMOFs **2** and **4**, respectively, the epoxidation rate appears to be limited by the intrinsic activity of the Mn-Salen catalytic units. The reactivity studies in the present isoreticular CMOF series thus make a convincing case that CMOFs can be effective heterogeneous asymmetric catalysts for a number of important organic transformations. The open channel size-dependent conversions observed for CMOFs **1**−**5** also provide indirect evidence for the reagents accessing active catalytic sites in the interiors of CMOF crystals and highlight the opportunity for size- and enantioselective catalysis with CMOFs.

It is difficult to obtain quantitative kinetic parameters from the present study since the reaction rate depends on the MOF crystal sizes as well as the stirring rate. Since most MOFs, including the present CMOF series, are mechanically unstable, they tend to fracture into smaller particles by the magnetic stir bar. The contribution from the surface catalytic sites can be a significant factor, which can lead to an underestimate of the dependence of the conversion on the CMOF open channel size. To eliminate the possibility of the catalytic activity all arising from surface catalytic sites of very small particles, epoxidation of **6d** was carried out with large crystals of CMOF-**4** ($\sim 0.4 \times 0.4 \times 0.4$ mm³ on average, 0.1 mol % catalyst loading) without stirring or shaking. A 35% conversion was obtained after 1 h, and the epoxide product exhibited 84% ee, clearly demonstrating the ability for the substrate to enter the interior of the MOF crystals, since such large crystals possess too few surface catalytic sites to account for the reaction. In comparison, epoxidation of **6d** with CMOF-**1** crystals ($\sim 0.3 \times 0.3 \times 0.3$ mm³ on average, 0.1 mol % catalyst loading) under the same conditions gave 10% conversion at 78% ee, consistent with the less accessible catalytic sites inside smaller open channels of CMOF-**1**. These results provide unambiguous evidence for the alkenes and oxidants to access the catalytic Mn-Salen sites in the interiors of these MOF crystals.

We have also carried out a number of control experiments to demonstrate the heterogeneity of CMOF catalysts. First, a supernatant of CMOF-**4** after sonication was used to catalyze the epoxidation of **6d** with 1 equiv of the oxidant, but no epoxide was observed. Second, we tested the reactivity of the supernatant after epoxidation reaction in a crossover experiment. Substrate **6e** was epoxidized in the presence of the CMOF-**4** catalyst with gentle shaking (instead of stirring) in 1 h to afford the epoxidation product in 57% conversion and 74% ee. The solid was removed from the reaction mixture by filtering through Celite, and a second substrate, **6d**, and 2 equiv of the oxidant were then added to the supernatant. After 3 h, no epoxidation was detected by GC. This lack of epoxidation in the crossover experiment strongly supports the heterogeneous nature of the CMOF catalysis.

We have also examined the recyclability of CMOF-**5** and CMOF-**4** for the asymmetric epoxidation of **6b** and **6c**, respectively. As shown in Table 3, CMOF-**4**/CMOF-**5** was readily recovered from the catalytic reaction via centrifugation, and the recovered catalyst showed only slight deterioration in conversion and enantioselectivity. Furthermore, the solid catalyst recovered from the catalytic epoxidation reaction catalyzed by CMOF-**5** exhibited the same PXRD as the pristine solid of CMOF-**5** (Figure 6), unambiguously supporting the stability of the CMOF framework during the catalytic reactions. Inductively coupled plasma mass spectrometric (ICP-MS) analysis of the supernatant showed that less than 7.5% of the manganese had leached into

Table 3. Recycling of CMOF-**4** and CMOF-**5** for the Asymmetric Epoxidation

X = -CN for CMOF-**4** and = -H for CMOF-**5**

	run	conversion, %[b]	ee, %[c]
CMOF-**4**	1	78	76
	2	80	72
	3	79	71
	4	72	69
CMOF-**5**	1	72	86
	2	70	81
	3	62	80

[a] The reactions were carried out with 0.5 mol % catalyst and 0.5 equiv of oxidants. [b] Determined by GC. [c] Determined by chiral capillary column supelco β-DEX 120.
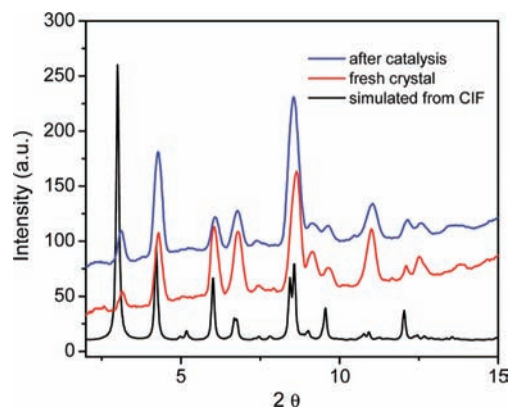

Figure 6. PXRD patterns of CMOF-**5**: simulated from CIF file (black), pristine CMOF-**5** (red), and CMOF-**5** recovered from the epoxidation reaction (blue).

the reaction mixture when the epoxidation was carried out in the presence of 0.1 mol % CMOF-**5** catalyst.

MOFs based on the [Zn$_4$O(carboxylate)$_6$] SBUs have been shown to be hydrolytically unstable.[70] This intrinsic instability sets the limit of the applications of the present CMOFs in enantioselective alkene epoxidation reactions. More commonly used oxidants m-CPBA and bleach were attempted for the epoxidation reactions, but the CMOFs were found to be unstable under the reaction conditions required for these oxidants. The discussion of the stability of a certain catalyst has to be specific to reaction conditions. We have demonstrated that CMOFs **1**−**5** function as efficient heterogeneous asymmetric alkene epoxidation catalysts with 2-(*tert*-butylsulfonyl)iodosylbenzene as oxidant.

Conclusion

A family of isoreticular chiral MOFs was rationally designed and synthesized by direct incorporation of well-defined Mn-Salen catalysts into the frameworks. The open channel sizes in

this CMOF series were systematically tuned by introducing spacers of different lengths, as well as by successful control over framework catenation. These isoreticular chiral MOFs were demonstrated to be highly active in catalyzing enantioselective alkene epoxidation reactions. The isoreticular nature of this CMOF series also allows probing the dependence of epoxidation reaction rates on the open channel dimensions. The rates of epoxidation reactions strongly depend on the CMOF open channel sizes, providing solid evidence that larger open channel dimensions can increase reaction rate by facilitating the diffusion of reactant and product molecules. The catalytic activities of CMOFs **2** and **4** rival that of a homogeneous control catalyst, suggesting the catalytic activity of the CMOFs with large open channels is limited by the intrinsic reactivity of the catalytic molecular building blocks. The CMOF catalysts are recyclable and reusable and retain their framework structures after epoxidation reactions. The modular nature of this synthetic approach should allow the design of other metal-Salen-based MOF catalysts for many important asymmetric organic transformations.

Experimental Section

General experimental section and detailed procedures for ligand and CMOF synthesis and characterization are provided in the Supporting Information. Only key representative experimental procedures are shown below.

A typical procedure for crystal growth: Zn$_4$O(**L$_2$**)$_3$·(DEF)$_{37}$·(EtOH)$_{23}$·(H$_2$O)$_4$ (CMOF-**4**): **L$_2$**-H$_2$ (10 mg, 0.015 mmol) and Zn(NO$_3$)$_2$·6H$_2$O (10 mg, 0.034 mmol) were added to a 2-dram, screw-capped vial. DMF (3 mL) and EtOH (2 mL) were then added. The vial was capped and placed into an oven at 60 °C for 12 days. Black cubic crystals were obtained after filtration (19.1 mg, 54% yield). Solvent content calculated from proposed formula: DEF, 52.5%; EtOH, 14.8%; H$_2$O, 1.0%. Determined by ^{1}H NMR/TGA: DEF, 52.3%; EtOH, 14.9%; H$_2$O, 0.9%.

General procedure for the enantioselective epoxidation reaction of alkene: CMOF-**5** (1.08 mg, 0.0006 mmol) was charged into a 2-dram, screw-capped vial, washed with CH$_2$Cl$_2$ three times, and sonicated for 10 min. To this vial were added alkene (0.6 mmol), undecane (0.063 mL, 0.3 mmol), and CH$_2$Cl$_2$ (0.5 mL). 2-(*tert*-Butylsulfonyl)iodosylbenzene (0.010 g, 0.03 mmol) was then added. The same amount of oxidant was added nine more times at 15 min intervals. Aliquots of the reaction solution were taken (10 µL), diluted with EtOAc and filtered through a syringe filter. The filtrate was analyzed by GC to give the conversion and enantioselectivity.

Slightly modified procedures are used for time-dependent conversion, heterogeneity test, crossover catalysis, CMOF recycle and reuse, catalyst framework stability, and catalyst leaching studies. All of these details are provided in the Supporting Information.

Supporting Information Available: General experimental section; procedures for ligand synthesis; synthesis and characterization of isoreticular CMOFs; single-crystal X-ray structure determinations; representative procedure for dye uptake measurements; CMOF-catalyzed enantioselective epoxidation reactions of unactivated alkenes. This material is available free of charge via the Internet at http://pubs.acs.org.

JA1069773

(70) Low, J. J.; Benin, A. I.; Jakubczak, P.; Abrahamian, J. F.; Faheem, S. A.; Willis, R. R. *J. Am. Chem. Soc.* **2009**, *131*, 15834.